Subleading properties of the QCD flux-tube in 3-d lattice gauge theory

Pushan Majumdar

(Department of Theoretical Physics, Indian Association for the Cultivation of Science, Jadavpur, Kolkata)

In collaboration with N.D. Hari Dass, Bastian B. Brandt

Yoshiaki Koma & Miho Koma

Intoduction

- Mechanism of Confinement : On the lattice there is evidence of flux tube formation.

- Conjecture : Flux tube $\equiv$ bosonic string.

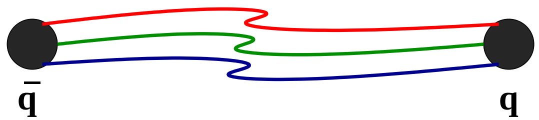

- Effective theories for flux tubes (hadronic strings) .

  Write down most general (series) action with vanishing conformal anomaly in any dimension. (Polchinski & Strominger)

  Write down action as a series in $1/r$ (r : length of flux tube) and impose open-closed duality. (Lüscher & Weisz)

- Zero-mass fluctuations of the string $\longrightarrow$ power corrections to static quark potential
  Coefficient of leading correction: Universal & One loop exact: Lüscher term - value $= -\frac{(d-2)\pi}{24}$
  This is reproduced by all effective theories at leading order.

- Need to go to sub-leading order to distinguish between different string models.

- Can we identify the scale at which string-like behaviour of the flux tube sets in?

Observables on the lattice

- Polyakov loop correlators:
  Accurate ground state energy.

$$\langle P^{\dagger}P(r)\rangle = \sum_{i=0}^{\infty} b_i \,\exp[-E_i(r)N_t]$$

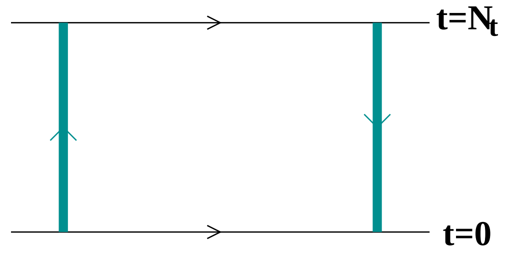

Polyakov Loop correlator

- Wilson loops :
  Suitable for excited states

$$W(r,\Delta T) = \sum_{\alpha} \beta_i^{\alpha}\beta_j^{\alpha} e^{-E_\alpha(r)\Delta T}$$

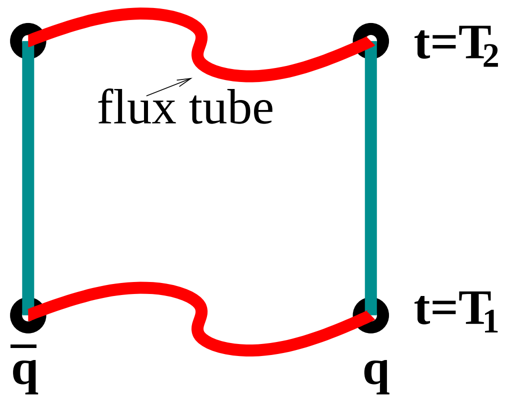

Wilson Loop

- The string pictures holds at large r $\Rightarrow$ large loops.

- Note that $W(r, \Delta T) \propto \exp(-r\Delta T)$

- Since we need large r, we must either work with small ΔT, or have the means to extract exponentially suppressed signals from the noise.

- 1st alternative has been followed by Kuti *et.al.* using asymmetric lattices and a very large number of basis states.

- Advances in algorithms (e.g. multilevel schemes) and computing power now allow for exponential error reduction and reliable extraction of expectation values of large Wilson loops.

- Some of the applications :

  1. Ground state of the flux tube.
  2. Excited states of the flux tube.
  3. Profile of the flux tube.
  4. Breaking of the flux tube.
  5. 3-quark potential.
  6. Glueball spectrum in SU(3) & U(1).
  7. Energy momentum tensor of the gluonic field.

Algorithm - Ground State

- $a \otimes b =$ T1(2,2,2,2)

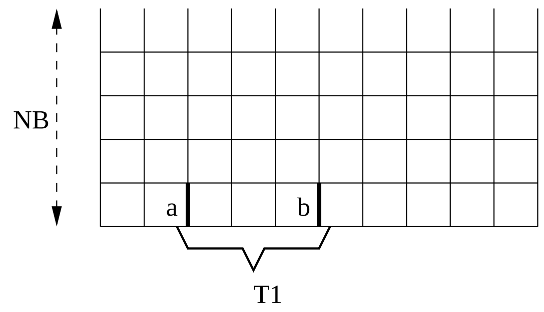

- $(\mathrm{T1})_{ijkl}(\mathrm{T2})_{jmln}$=$(\mathrm{Tp1})_{imkn}$ Averaging is carried out for Tp1.

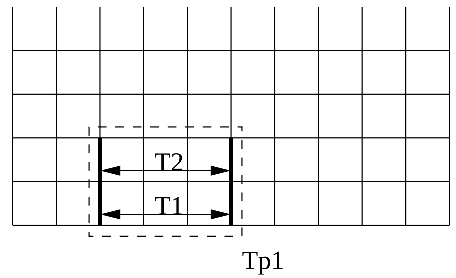

- The averaged Tp's are multiplied together to form the averaged propagator Tf.

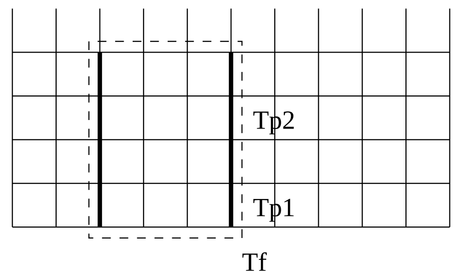

- L1, L2 & Tf are multiplied together to produce the Wilson loop.

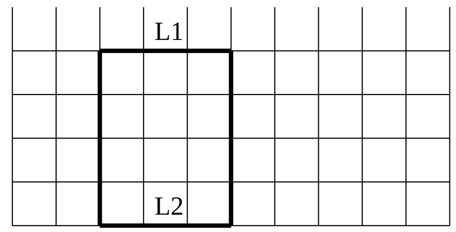

Important parameters of the algorithm : time slice thickness - Tp1 & the number of sublattice updates $iupd$.

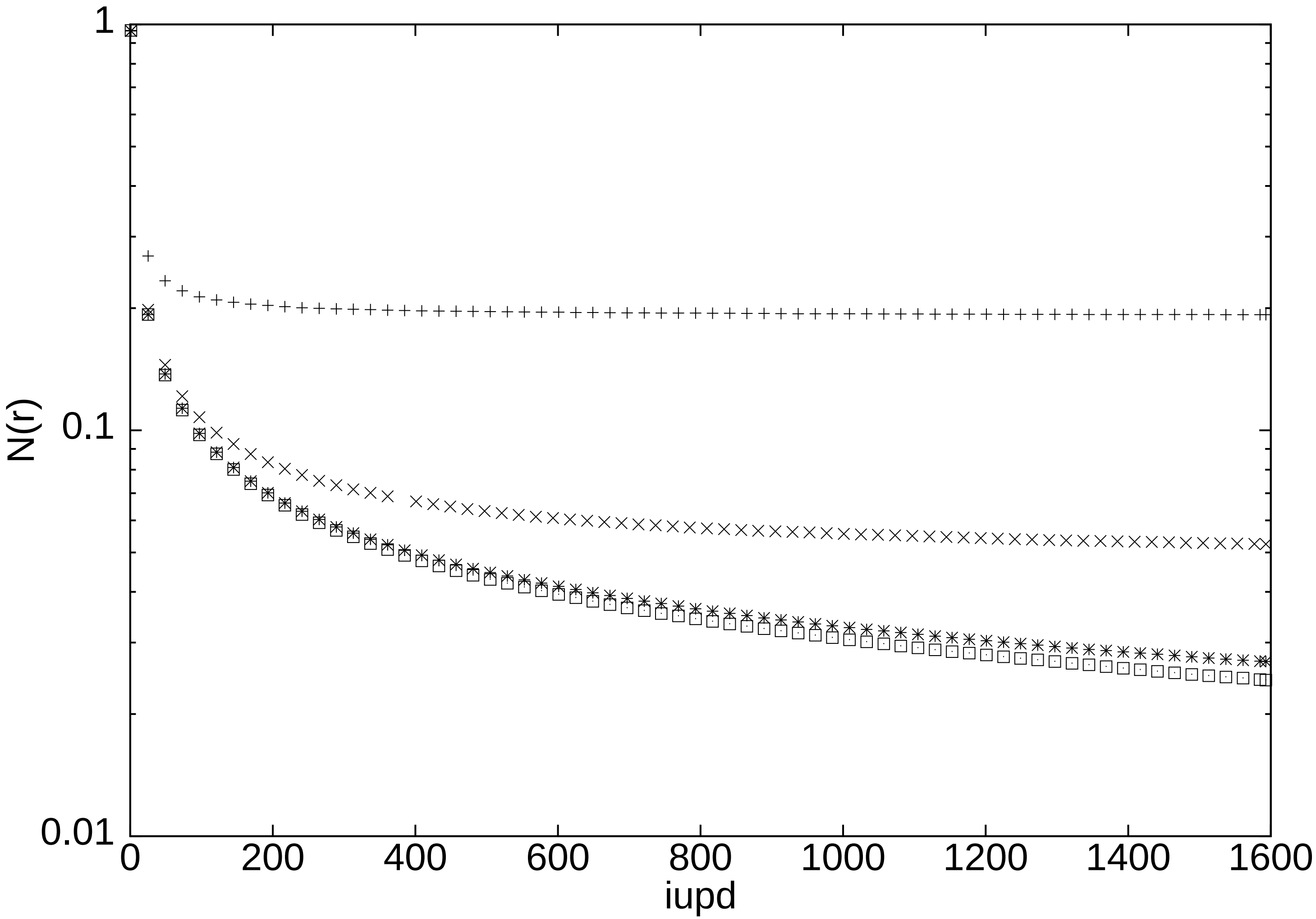

2-link norm vs $iupd$ for r=2,4,6 and 8 at $\beta = 3$

- Potential between static $q\bar{q}$ pair: (series in r^{-n})

$$V(r) \sim \sigma r + \widehat{V} - c/r + \cdots$$

Arvis : Ground state of Nambu-Goto string :

$$V_{\text{Arvis}} = \sigma r \left(1 - \frac{(d-2)\pi}{12\sigma r^2} \right)^{1/2}$$

Potential turns complex at $r = r_c$ (tachyons).

We look at the first and a scaled second derivative of $V(r)$.

$$f(\bar{r}) \; = \; V(r) - V(r-1) \qquad \text{with} \quad \bar{r} = r + \frac{a}{2} + \mathcal{O}(a^2)$$

$$c(\tilde{r}) \; = \; \frac{\tilde{r}^3}{2}[V(r+1) + V(r-1) - 2V(r)] \quad \text{with} \quad \tilde{r} = r + \mathcal{O}(a^2)$$

$\bar{r}$ & $\tilde{r}$ reduce lattice artefacts.

String predictions (d=3)

$$\text{L.O.}\ f(r) = \sigma + \left(\frac{\pi}{24}\right)\frac{1}{r^2} \qquad c(r) = -\frac{\pi}{24}$$

$$\text{N.L.O.}\ f(r) = \sigma + \left(\frac{\pi}{24}\right)\frac{1}{r^2} + \left(\frac{\pi}{24}\right)^2\frac{3}{2\sigma r^4} \qquad c(r) = -\frac{\pi}{24}\left(1+\frac{\pi}{8\sigma r^2}\right)$$

$$\text{Arvis}\ f(r) = \sigma\left(1-\frac{\pi}{12\sigma r^2}\right)^{-1/2} \qquad c(r) = -\frac{\pi}{24}\left(1-\frac{\pi}{12\sigma r^2}\right)^{-\frac{3}{2}}.$$

Perturbation theory

$$V_{\text{pert}}(r) = \sigma_{\text{pert}} r + \frac{g^2 C_F}{2\pi}\ln g^2 r + (\text{higher order terms}) \qquad (1)$$

$\sigma_{\text{pert}} = \frac{7g^4 C_F C_A}{64\pi}$ with $C_F = 3/4$ and $C_A = 2$.

β	r_0/a	r values	lattice	iupd	# of meas.
5.0	3.9536(3)	$2-8$	36^3	16000	1600
(ts=2)		$7-9$	40^3	32000	3200
		$8-12$	48^3	48000	20800
7.5	6.2875(10)	$4-8$	48^3	8000	1100
(ts=4)		$7-12$	64^3	18000	1100
		$11-16$	64^3	36000	7200
		$13-17$	64^3	48000	6700
10.0	8.6022(8)	$2-7$	48^3	16000	2850
(ts=4)		$6-9$	48^3	16000	200
		$8-14$	84^3	24000	1100
		$13-19$	84^3	36000	2250
12.5	10.916(3)	$2-9$	48^3	16000	2700
(ts=6)		$8-14$	72^3	24000	1150

$r_0^2 f(r)$ vs r/r_0

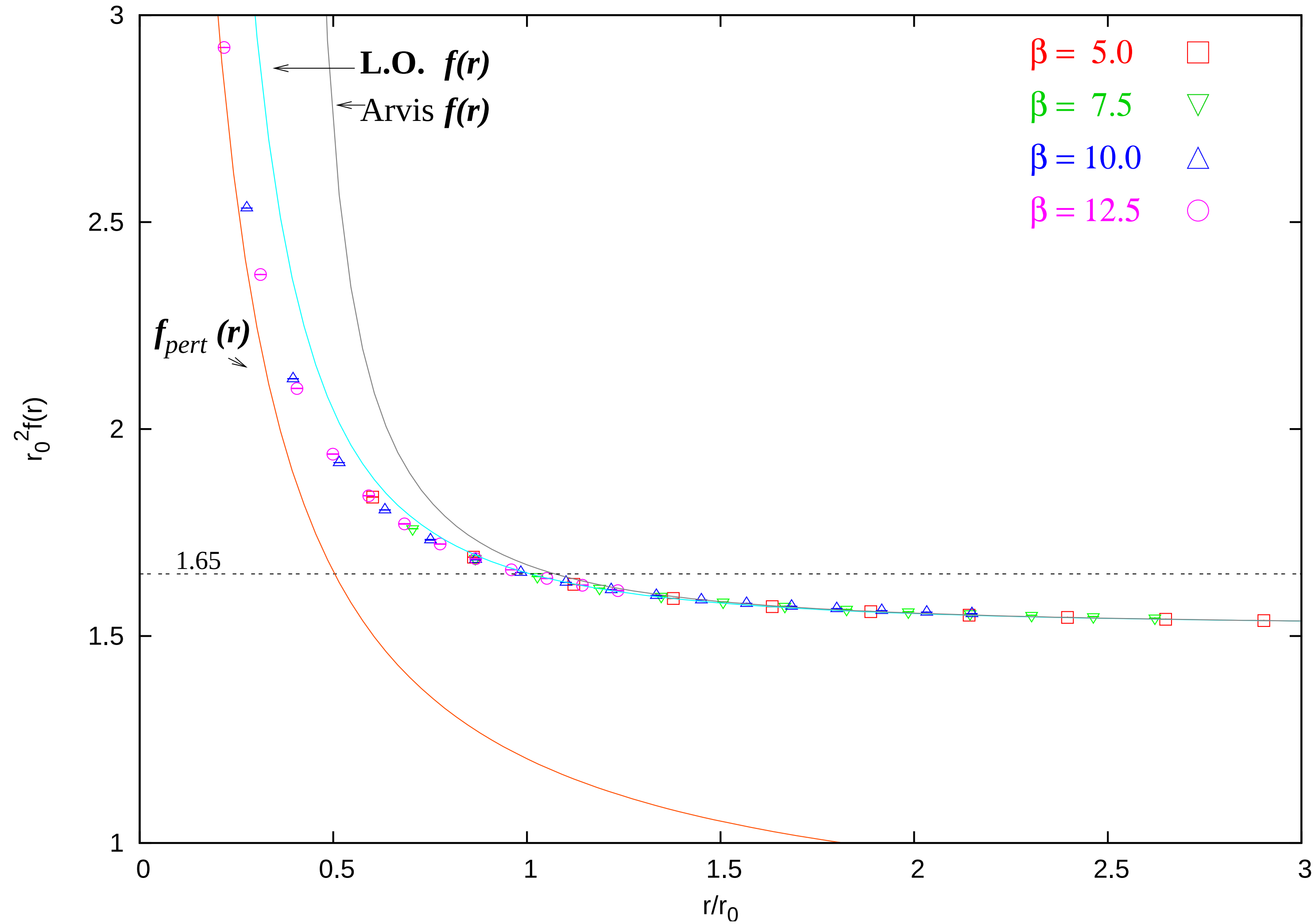

$f_{\text{pert}}(r)$: 1-loop perturbation theory.

Dotted line : $r_0^2 f(r) = 1.65$, locates the Sommer scale.

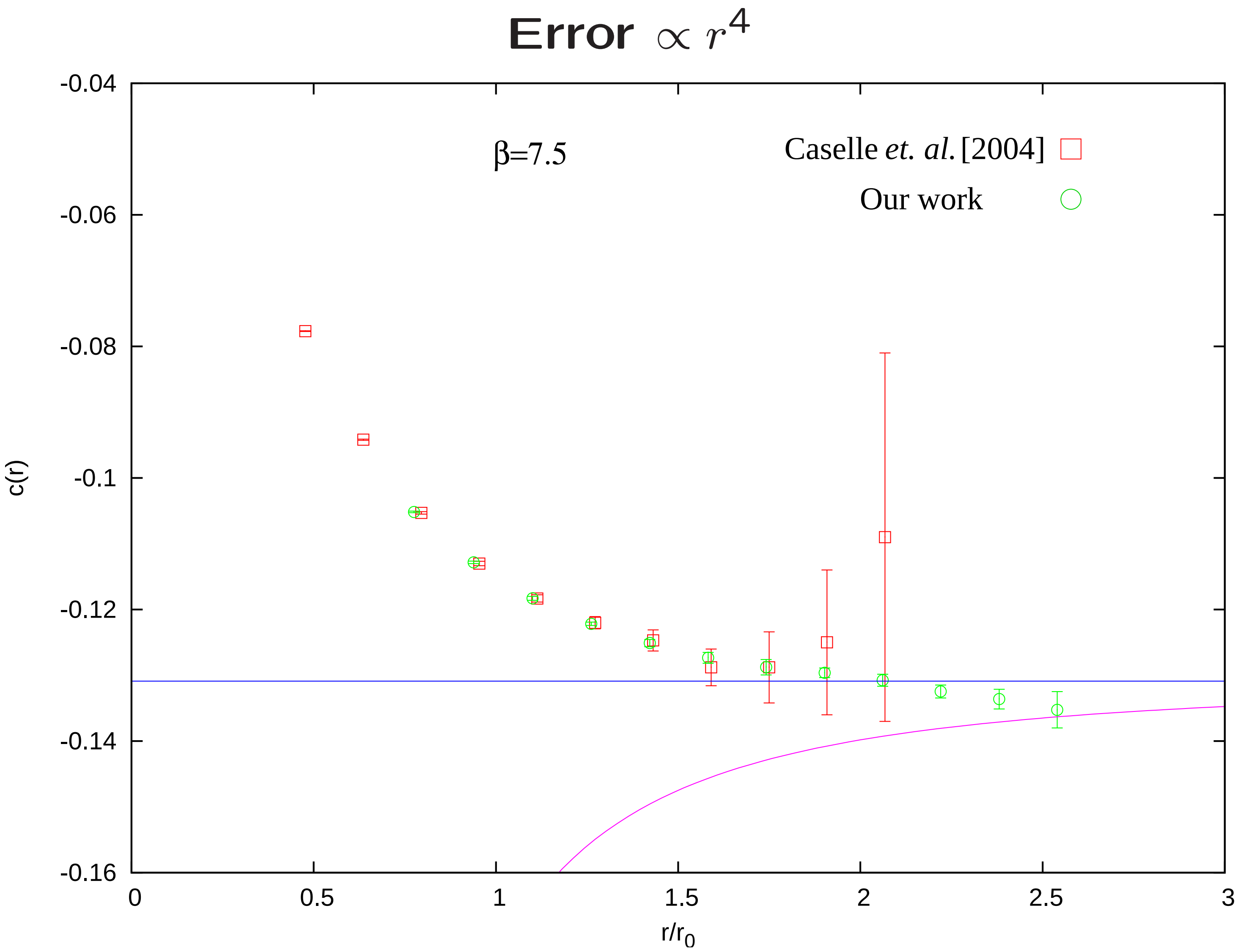

Error $\propto r^4$
β=7.5
Caselle et. al. [2004]
Our work
c(r)
r/r0
-0.04
-0.06
-0.08
-0.1
-0.12
-0.14
-0.16
0
0.5
1
1.5
2
2.5
3

$c(\tilde{r})$ vs r/r_0

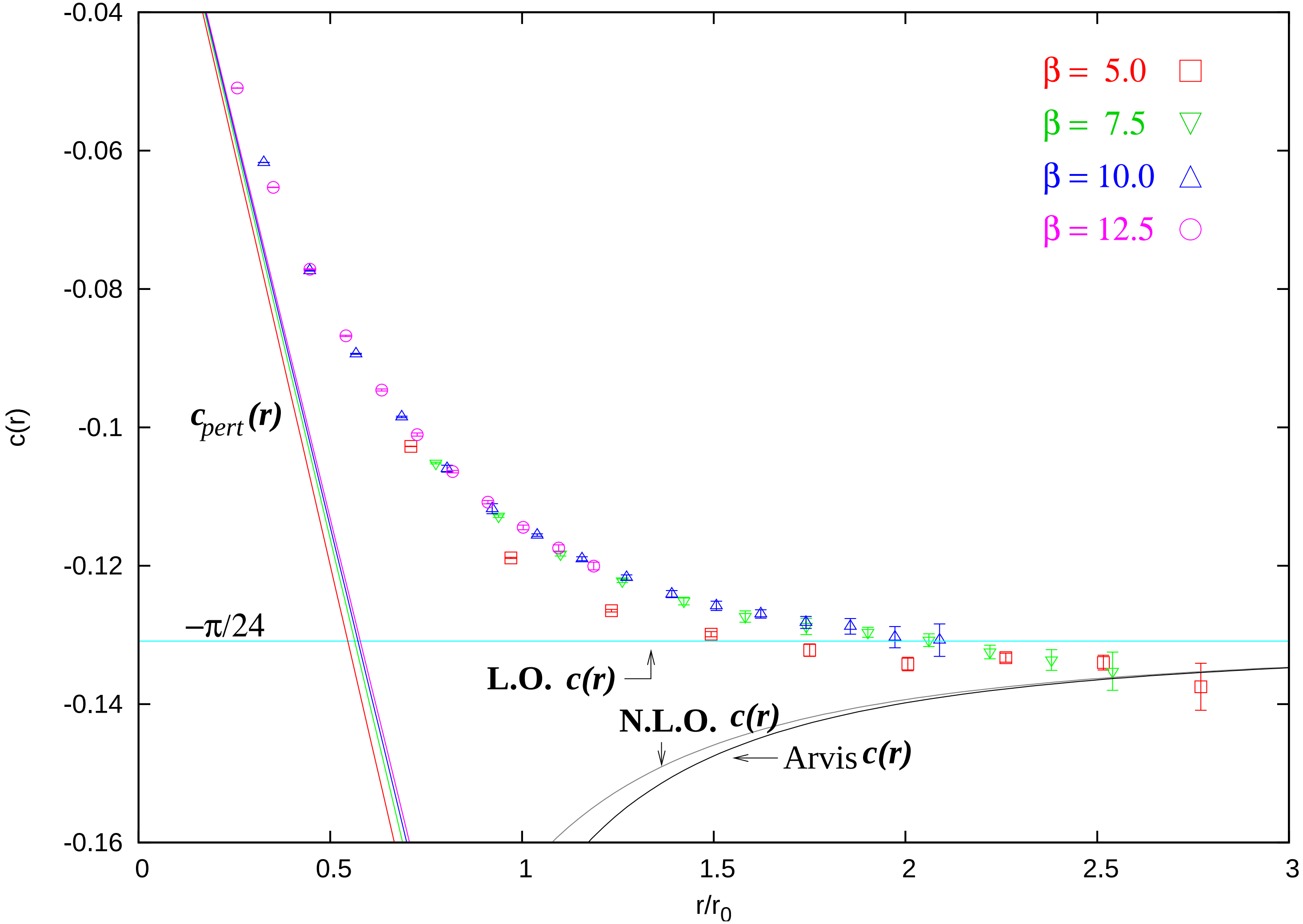

$c_{\text{pert}}(r)$: 1-loop perturbation theory with $\beta = 12.5$ closest to data and $\beta = 5$ farthest.

Interpolating curves

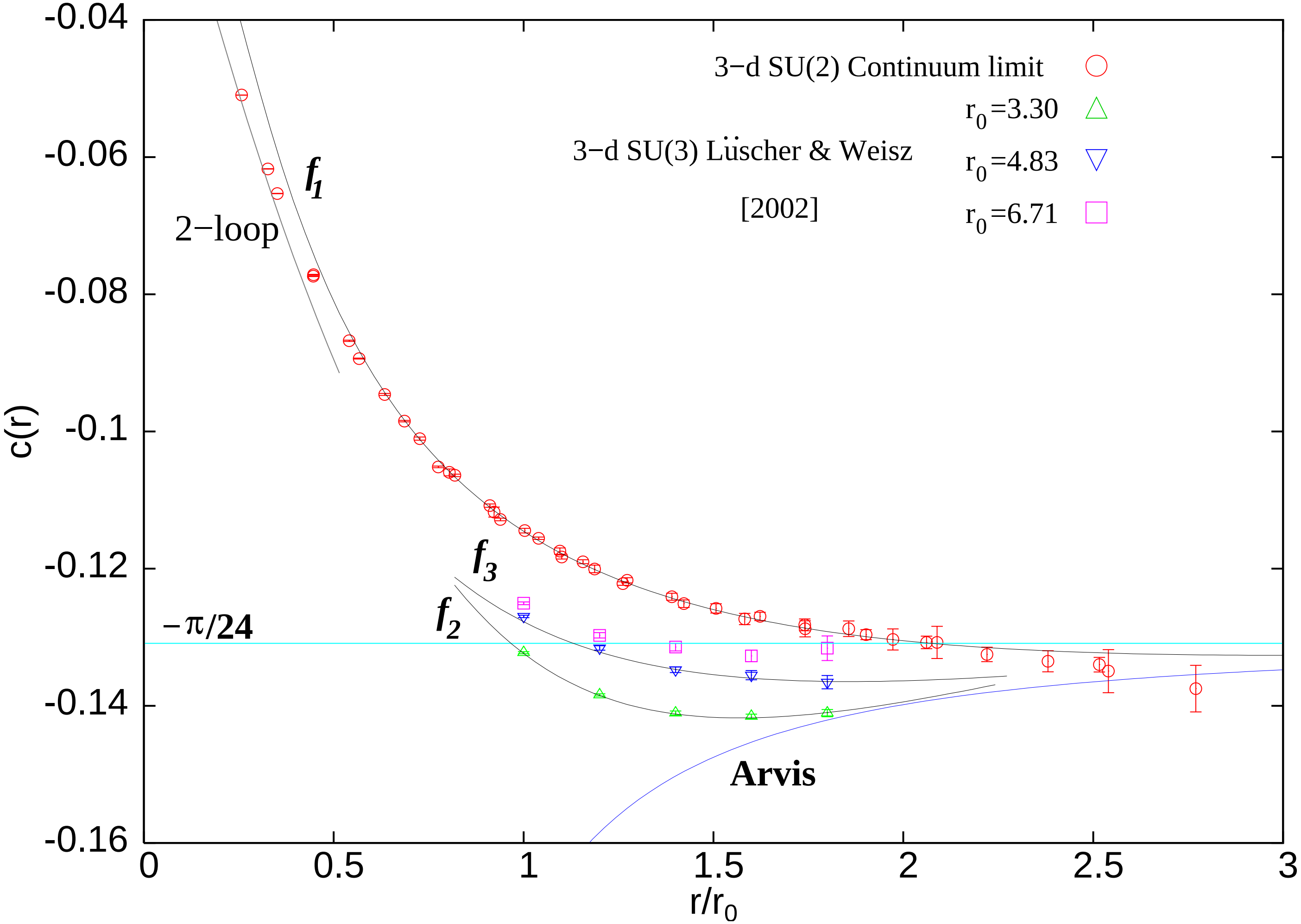

f_1, f_2 & f_3 are of the form $a\left(x^{-2n}-x^{-n}+bx^{-3n}\right)$ with (a,b,n) $(0.444,-0.258,0.357)$, $(0.458,-0.289,0.691)$ & $(0.442,-0.287,0.498)$.

2-loop : $-\frac{g^2 r_0 C_F}{4\pi}\frac{r}{r_0}+\frac{Ag^4 r_0^2}{2}\left(\frac{r}{r_0}\right)^2$ with $A=0.013162$.

Excited states of the flux tube

Behaviour under charge conjugation and parity – **CP**

P: Reflect in $q\bar{q}$ axis : $x(\kappa) \longrightarrow -x(\kappa)$

C: Interchange q and $\bar{q}$: $x(\kappa) \longrightarrow x(r-\kappa)$

Combinations $\Leftrightarrow$ symmetry channels.

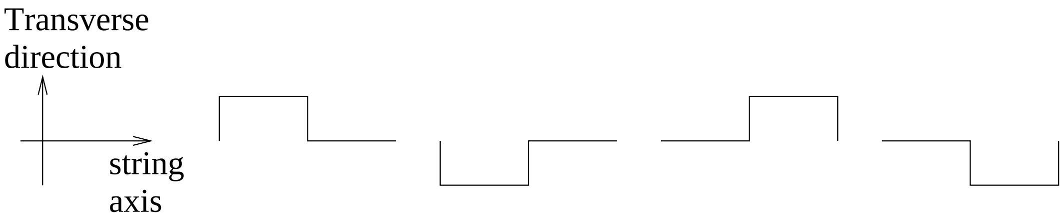

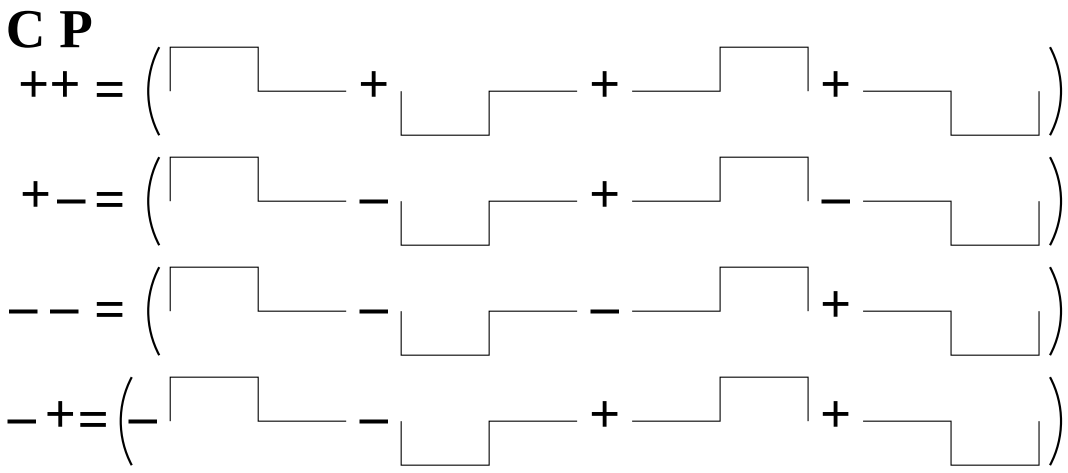

Algorithm - Excited states

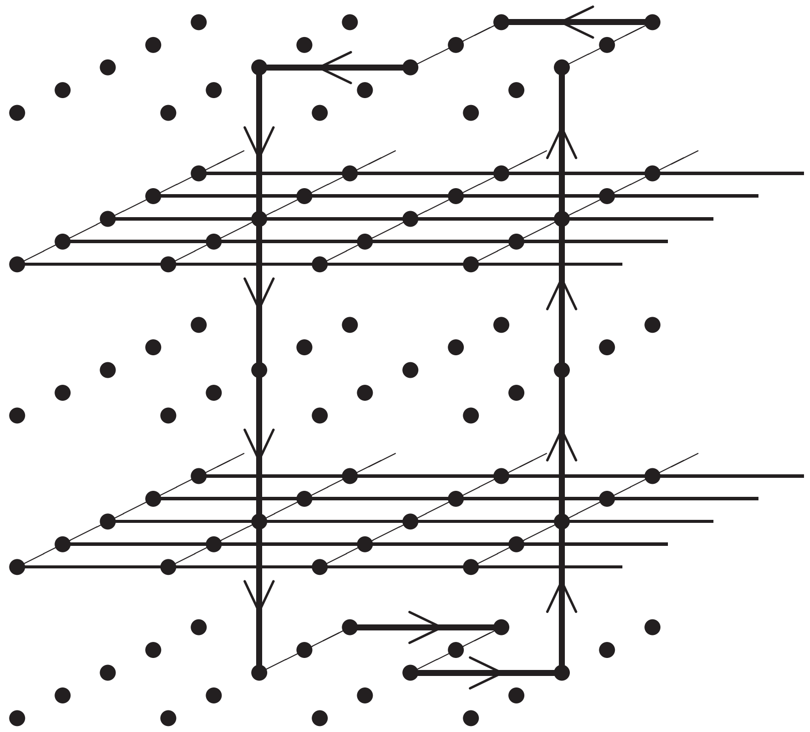

A wilson-loop with different sources at the ends, that lie in the middle of the time-slices. The slices with the solid lines are the time slices with fixed lines during the sublattice updates.

r	W_1 New	W_1 Old	W_2 New	W_2 Old	W_3 New	W_3 Old
4	0.44	0.15	2.7	7.0	9.2	100
5	0.63	0.21	2.7	8.3	8.6	100
6	0.86	0.28	2.7	4.5	8.8	100
7	1.1	0.35	2.9	7.3	8.8	100
8	1.4	0.45	3.1	5.5	9.5	100
9	1.7	0.56	3.6	10	11	100
10	2.1	0.74	4.2	11	14	100
11	2.7	1.0	5.8	27	22	100
12	3.5	1.7	8.6	88	44	100

Percentage errors for Wilson loops for energies E_1, E_2 and E_3. $\beta = 5$, $T = 8$ with r varying between $4-8$. Time $\approx$ 1100 mins.

Old method: 730 mesurements with no source averaging.

New method: 50 mesurements with 12000 updates for source averaging.

2-link averaging was same for both methods.

Energy of the string excited states

$$\textbf{L.O.}\quad E_n = \sigma r + \mu + \frac{\pi}{r}(n - \frac{d-2}{24})$$

$$\textbf{N.L.O}\quad E_n = \sigma r + \mu + \frac{\pi}{r}(n - \frac{d-2}{24}) - \frac{\pi^2}{2\sigma r^3}(n - \frac{d-2}{24})^2$$

$$\text{Arvis}\quad E_n = \sigma r(1 + \frac{2\pi}{\sigma r^2}(n - \frac{d-2}{24}))^{1/2}$$

We will look mostly at the energy difference $E_n - E_m$.

Correction factors

$$\lambda(T) = \alpha_1 e^{-ET}\left(1 + \frac{\alpha_2}{\alpha_1}e^{-\delta T}\right)$$

$$-\frac{1}{T_2 - T_1}\log\frac{\lambda(T_2)}{\lambda(T_1)} = \bar{E} + \frac{1}{T_2 - T_1}\left[\frac{\alpha_2}{\alpha_1}e^{-\delta T_1}\left(1 - e^{-\delta(T_2 - T_1)}\right)\right].$$

Excited state energies at $\beta = 5$ and $\beta = 7.5$.

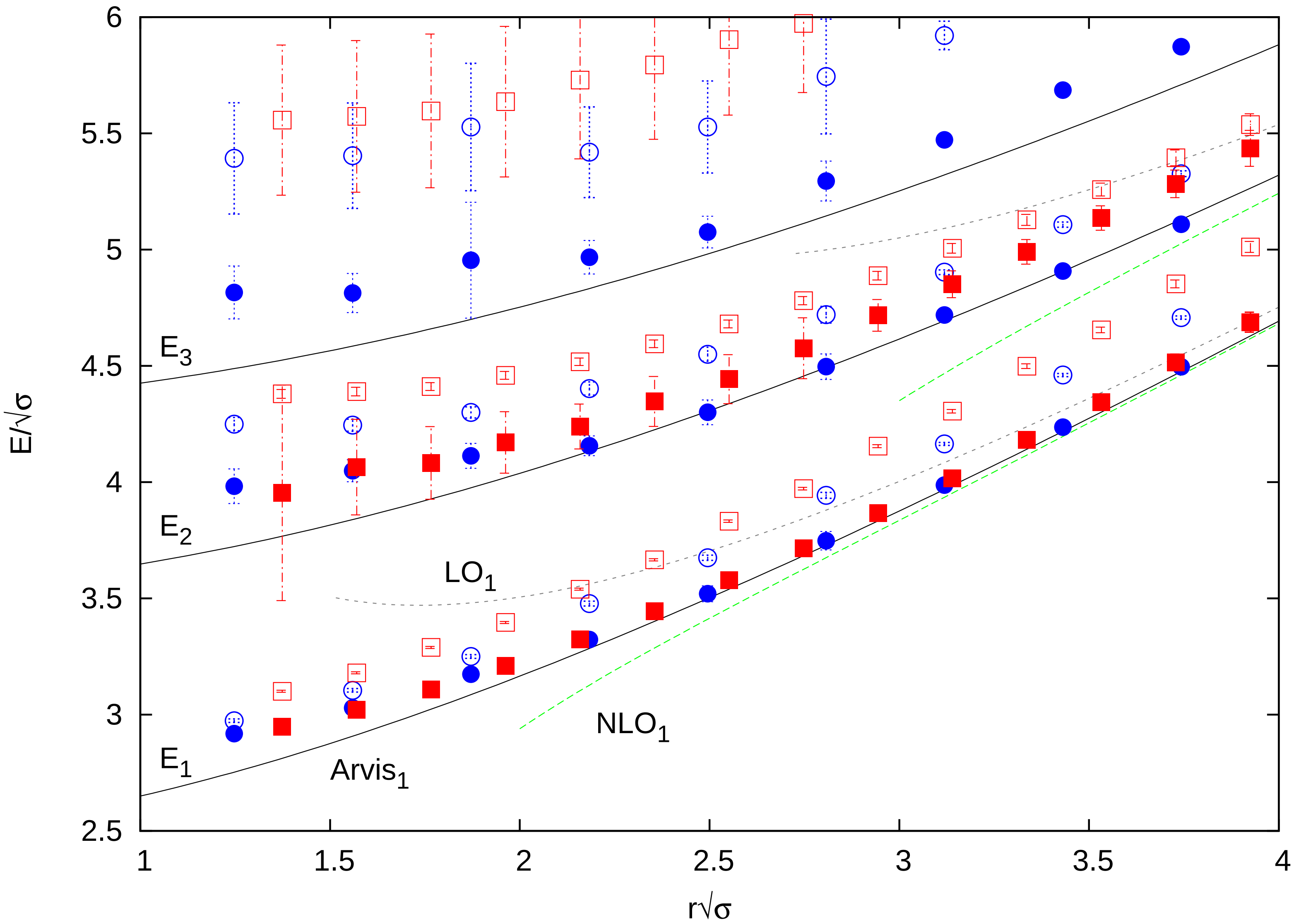

Open symbols : naive values

Filled symbols : corrected values.

Energy difference at $\beta = 5$ and $\beta = 7.5$.

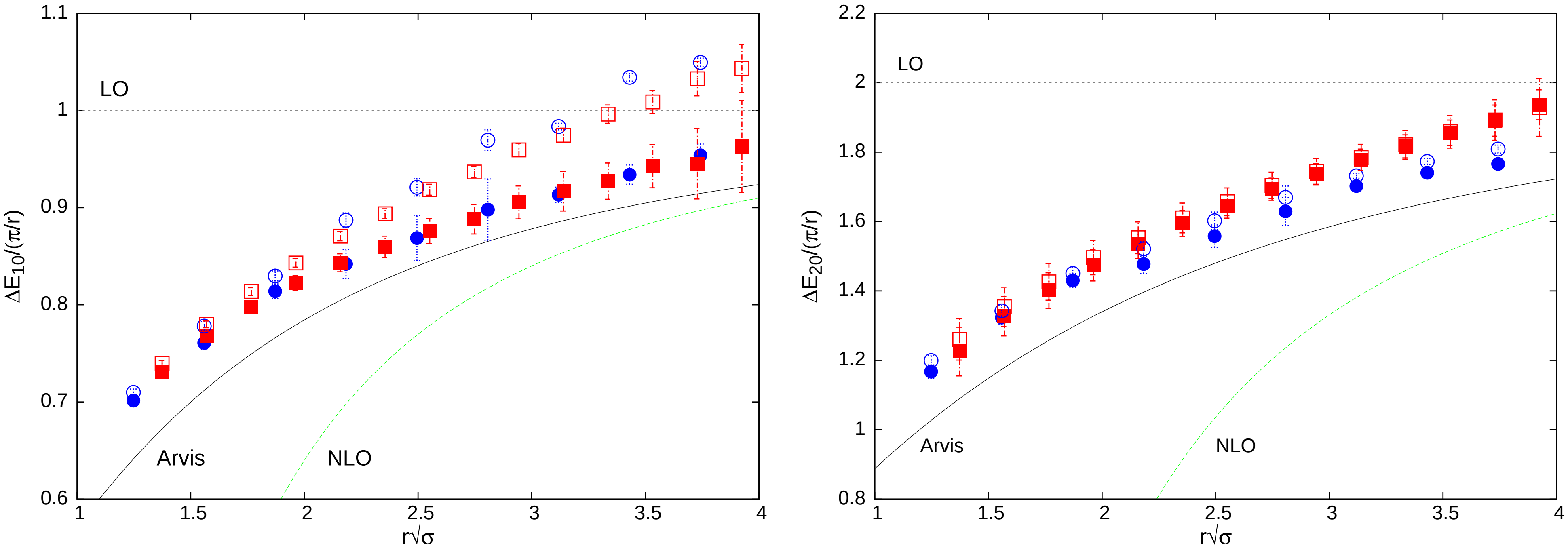

The distance corresponding to $r\sqrt{\sigma} = 4$ is about 1.6 fermi.
At $r\sqrt{\sigma} = 4$ and ΔE_{10} the difference between the **L.O.** and Arvis curves are $< 10\%$. For ΔE_{20} the difference is about 20%.
For ΔE_{20} at $\beta = 7.5$, the corrections are still not fully under control.

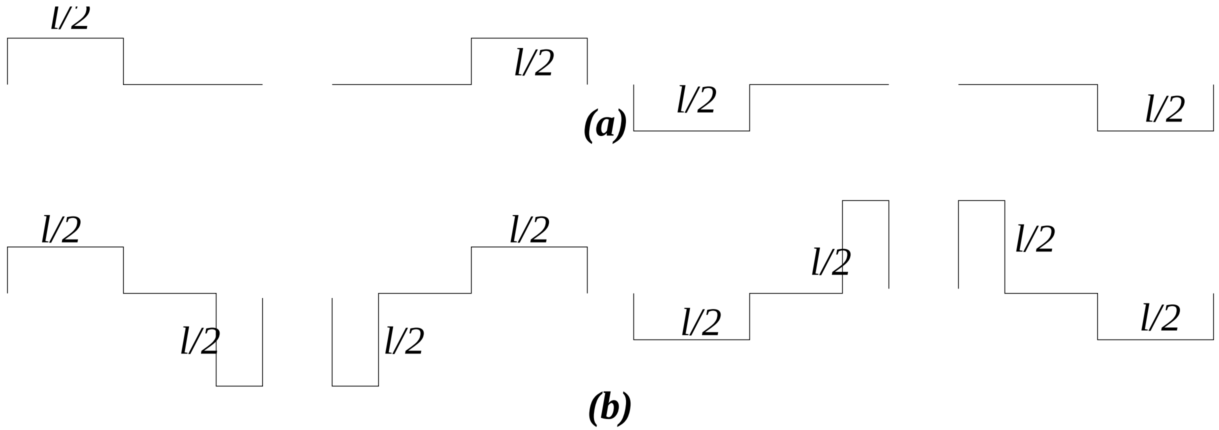

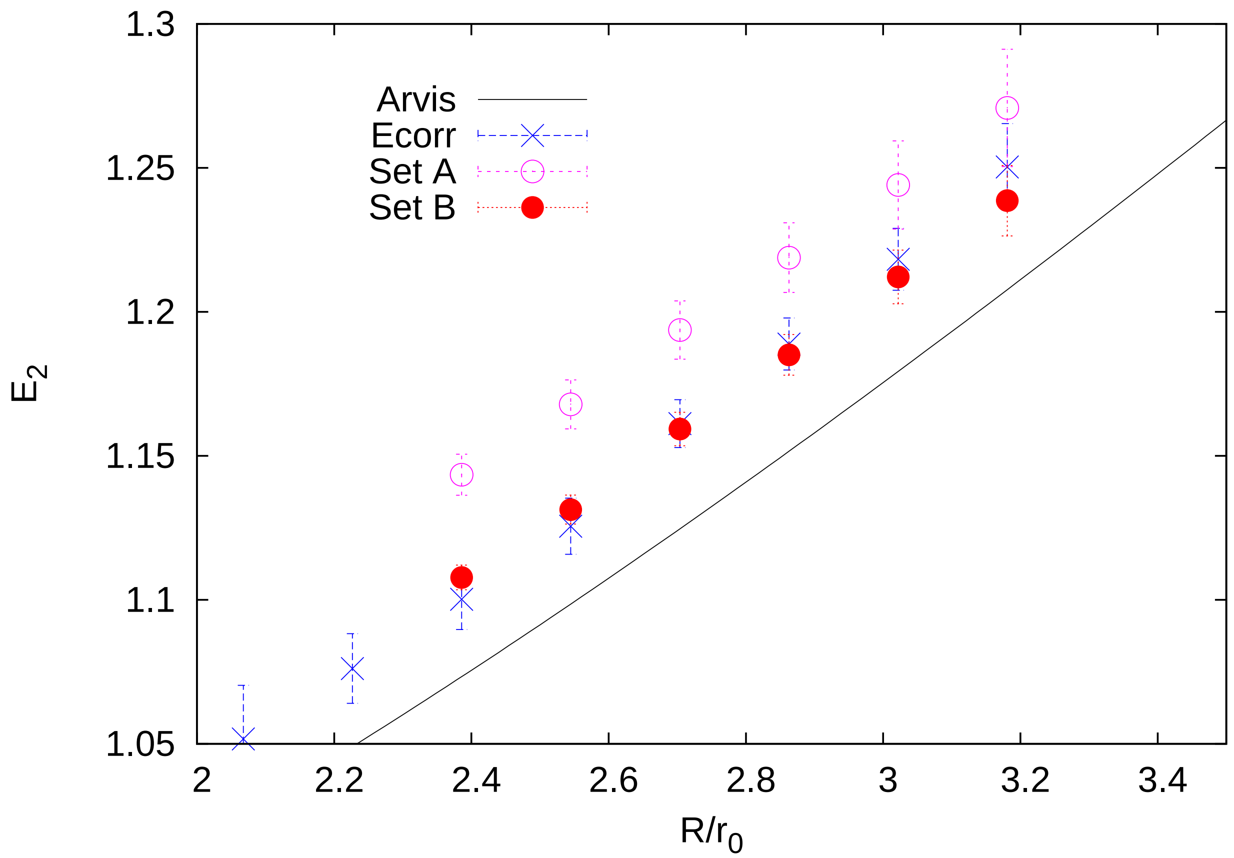

E_2 requires a better "wave function" as we approach continuum limit.

Used source (b) to couple strongly to E_2.

Plot shows E_2 values using source (a) and (b).

Values using (b) coincide with the corrected values from (a), but have lower error bars.

Flux tube profile

- Distribution of electric field in flux tube
  a) thickness of flux-tube
  b) parameters for effective theory (dual superconductivity)

- $\langle \mathcal{O} \rangle = \frac{\langle P^* P \mathcal{O} \rangle}{\langle P^* P \rangle} - \langle \mathcal{O} \rangle$
  eg: Electric Field : $\mathcal{O}_E(n) = i\bar{\theta}_{\mu\nu} = i(\theta_{\mu\nu} - 2\pi n_{\mu\nu}(n))$

$$[P^*PO] = \frac{1}{3N_s^3(N_t/2)} \sum_{m_s,\, i}$$

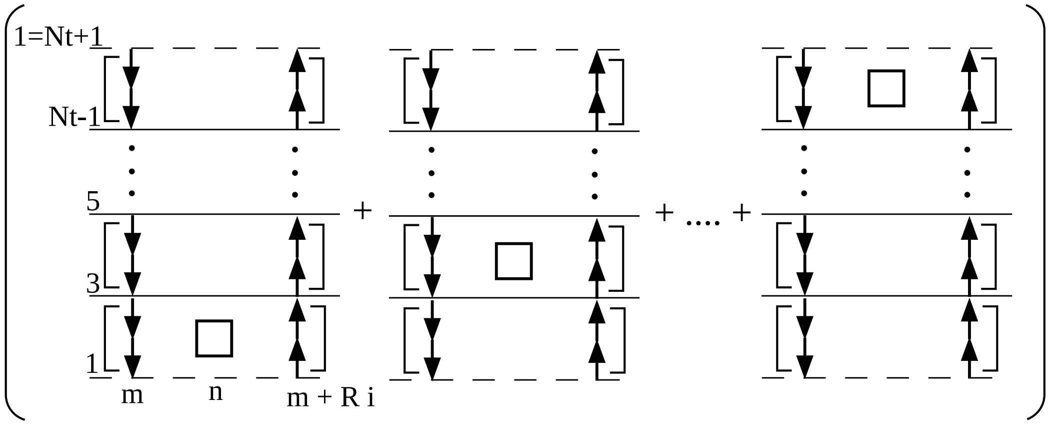

Conclusions

- For the Lüscher term, the asymptotic value is approached in a non-monotonic way with r.

- 1-loop perturbation theory holds upto distances of 0.1 fermi.

- Almost impossible to distinguish the type of the string from the force data.
  Differences are at the level of 0.1% at about $2r_0$.

- $c(r)$ suggests that a Nambu-Goto like behaviour is good beyond $2.5r_0$.

- Onset of string behaviour seems to be pushed towards larger r as one approaches the continuum.

- We have found a way to use the multilevel philosophy for the excited states as well.

- It seems that we need to use both the multilevel technique as well as improved wave functions to go ahead. We have taken a first step to show how it can be done.

- We are finally in a position to start distinguishing between different string models as sub-leading effects become visible.